Polymer 52 (2011) 2032–2043

Contents lists available at ScienceDirect

Polymer

journal homepage: www.elsevier.com/locate/polymer

# Fundamental salt and water transport properties in directly copolymerized disulfonated poly(arylene ether sulfone) random copolymers

Wei Xie [a], Joe Cook [a], Ho Bum Park [b], Benny D. Freeman [a,*], Chang Hyun Lee [c], James E. McGrath [c]

[a] University of Texas at Austin, Center for Energy and Environmental Resources, 10100 Burnet Road, Building 133, Austin, TX 78758, United States
[b] WCU Department of Energy Engineering, Hanyang University, Seoul 133-791, South Korea
[c] Virginia Polytechnic Institute and State University, Macromolecules and Interfaces Institute, Blacksburg, VA 24061, United States

ARTICLE INFO

*Article history:*
Received 22 December 2010
Accepted 3 February 2011
Available online 21 March 2011

*Keywords:*
Disulfonated polysulfone
Transport properties
Desalination

ABSTRACT

Water and sodium chloride solubility, diffusivity and permeability in disulfonated poly(arylene ether sulfone) (BPS) copolymers were measured for both acid and salt form samples at sulfonation levels from 20 to 40 mol percent. The hydrophilicity of these materials, based on water uptake, increased significantly as sulfonation level increased. The water permeability of BPS materials in both the salt and acid forms increases more than one order of magnitude as sulfonation level increases from 20% to 40%, while NaCl permeability increases by two orders of magnitude. The water and salt diffusivity and permeability were correlated with water uptake, consistent with expectations from free volume theory. In addition, a tradeoff was observed between water/salt solubility, diffusivity, and permeability selectivity and water solubility, diffusivity and permeability, respectively. This finding suggests a water/salt permeability/selectivity tradeoff, similar to that operative in gas separation polymers, in this family of polymers.



## 1. Introduction

Reverse osmosis membranes for desalination are currently derived from two basic classes of polymers: cellulose acetate (CA) and crosslinked aromatic polyamides (PA) [1–5]. CA membranes are susceptible to microbiological attack and are limited to operate in a relatively narrow feed pH range; they also undergo compaction at high temperature and pressures [6]. In contrast, PA membranes exhibit better transport properties and are more stable over a wider range of pH than CA membranes. Indeed, aromatic polyamides have come to dominate the market for desalination membranes [3]. Nevertheless, polyamides, as well as other materials that have been explored for desalination, such as polyamidohydrazides and polyetherureas, have poor resistance to oxidizing agents such as chlorinated disinfectants [2,4,7,8], which are widely used to control biofouling and to provide protection against various diseases. The lack of chlorine tolerance of PA desalination membranes requires that chlorine removal steps must be added to desalination processes to protect PA desalination membranes from exposure to chlorine [9].

Poly(arylene ether sulfone) homopolymers are well-known thermoplastics with excellent thermal and mechanical properties as well as resistance to oxidation and acid catalyzed hydrolysis [10]. Without chlorine sensitive amide linkages [11], membranes based on poly(arylene ether sulfone) have high tolerance to chlorine exposure [12]. Moreover, poly(arylene ether sulfone)s are already widely used as the porous substructure in desalination membranes [2,4]. Such poly(arylene ether sulfones) are highly hydrophobic. However, they may be partially sulfonated, which increases their hydrophilicity to the point that they can serve as desalination membranes [13–15]. Several studies on the desalination properties of sulfonated polysulfones prepared using a post-polymerization sulfonation process have been reported [16–20].

However, post-polymerization sulfonation yields materials with limited levels of sulfonation; additionally, such materials become water-soluble at high sulfonation levels, and it is difficult to insure quantitative reproducibility of the sulfonation level [21–23]. Post-polymerization sulfonation, which places the sulfonic acid group ortho to the activated aromatic ether linkage, often causes undesirable side reactions that lead to molecular weight degradation and crosslinking [22]. Furthermore, only one sulfonic acid group, at most, can be added to each repeat unit using bisphenol-A-based polymers [22].

Recently, disulfonated poly (arylene ether sulfone) random copolymers (specifically 4,4′-biphenol-based polysulfone, abbreviated as BPS) have been synthesized utilizing a disulfonated monomer, 3,3′-disulfonate-4,4′-dichlorodiphenyl sulfone (SDCDPS) [24], to introduce hydrophilic ionic structures into these materials,

* Corresponding author. Tel.: +1 512 232 2803; fax: +1 512 232 2807.
*E-mail address:* freeman@che.utexas.edu (B.D. Freeman).

0032-3861/$ – see front matter © 2011 Elsevier Ltd. All rights reserved.
doi:10.1016/j.polymer.2011.02.006

resulting in tough, ductile, random copolymers with varying levels of hydrophilicity [21,25,26]. Disulfonation of the commercially available activated aromatic dihalide monomer, 4,4′-dichlorodiphenyl sulfone (DCDPS), results in sulfonic acid(or sulfonate) functionalization on both deactivated phenyl rings ortho to the chlorine atoms and meta to the electron withdrawing sulfone group. Thus, sulfonated polysulfone copolymers prepared by this route are more chemically stable than previous post-polymerization sulfonated polysulfones. This process also permits two sulfonate units to be placed on each repeat unit [21]. Post-polymerization sulfonation is a rigorous chemical process, which can have side reactions which result in chain scission and crosslinking in addition to sulfonation. These disadvantages are completely eliminated by using sulfonated monomers in direct copolymerization [22]. This affords several important advantages relative to post-polymerization sulfonation techniques: (1) the sulfonation level is highly reproducible and may be precisely controlled, (2) the undesirable side reactions accompanying post-polymerization sulfonation are eliminated, and (3) the location of the ionic groups is precisely controlled.

This study reports water and salt transport properties of a series of random copolymers of disulfonated poly(arylene ether sulfone)s in both salt form and acid forms. These random copolymers exhibit good tolerance to aqueous chlorine at both low and high pH [12,27]. Initial studies have reported some water and salt permeation properties [28]. This paper reports values for water uptake and permeability, salt solubility, diffusivity, permeability and salt rejection which are reported as a function of the sulfonation concentration. The results are interpreted using free volume models for salt and water transport in polymers, and correlations between salt and water transport properties and water uptake are highlighted.

## 2. Experimental

### 2.1. Film preparation

Disulfonated poly(arylene ether sulfone) random copolymers were prepared by direct aromatic nucleophilic substitution step polymerization, as reported previously [21,23], resulting in copolymers whose structure is shown in Fig. 1. The nomenclature used for the copolymers is BPS-X (sulfonate salt form) and BPSH-X (free sulfonic acid form), where X is the molar percentage of hydrophilic sulfone groups (i.e., SDCDPS) in the polymer as shown in Fig. 1. For example, BPSH-20 is a disulfonated BPS copolymer in the free acid form containing 20 mol% SDCDPS and 80 mol% non-sulfonated sulfone monomers.

Dense, uniform, freestanding films (20–40 micron in thickness) of these polymers were prepared by dissolving the polymer (in the salt sulfonate form) in N-dimethylacetamide (DMAc; Sigma–Aldrich, St. Louis, MO, USA; used as received) to form a 5 wt.% solution. Next, the polymer solution was filtered through a nominally 2 μm pore size filter (#SS-2F-2 & #SS–2F–K4-2, Swagelok, Solon, OH, USA). After filtering, the viscous solution was cast onto a clean glass plate. The cast films were first dried in an oven at 80 °C for 24 h followed by exposure to vacuum for 48 h at 110 °C to further remove residual solvent. Afterwards, the film was peeled from the glass plate and soaked in deionized water for at least 1 h before use to extract residual solvent. Additional studies were performed at longer soaking times to verify that the time of soaking did not influence the results. In this regard, Table 1 shows that, within the uncertainty of the measurements, permeability data obtained from samples soaked for only 1 h prior to beginning measurements and those soaked for 4 days were consistent. These samples are referred to as salt form films. To prepare films in the acid form, salt form films were boiled in 0.5 M sulfuric acid, which was diluted from 96 wt.% sulfuric acid (Fisher Scientific, Hampton, NH, USA; used as received), for 2 h, followed by 2 h of extraction in boiling deionized water to remove excess acid. Finally, the membranes were kept in deionized water until use. This procedure quantitatively converts the salt form of the polymer to the acid form [12]. These samples are referred to as acid form films to recognize that they were in the acid form before transport property measurements were undertaken. While these acid form films can undergo ion exchange when contacted with water containing salt [29], the salt and water transport properties of acid form samples are different from those of samples that were not subject to acidification, so we make this distinction in nomenclature. The differences in transport properties of acid and salt form films likely stem from sensitivity of these non-equilibrium, glassy polymers to their thermal processing history, and additional studies are underway in our laboratories to further elucidate the influence of processing history on salt and water transport properties because this provides another degree of freedom that can be used to tailor the water and salt transport properties.

Polymer density was measured using a density determination kit (Part # 238490, Mettler Toledo, OH, USA) and an analytical balance (Model AG 204, Mettler Toledo, OH, USA) at 25 °C. The dry polymer density, $\rho_P$, was calculated as follows: [30,31]

$$\rho_P = \frac{m_A}{m_A - m_L}\rho_0 \quad (1)$$

where $m_A$ is the film weight measured in air, $m_L$ is the film weight measured in a non-solvent, i.e., an auxillary liquid that does not swell the polymer, and $\rho_0$ is the density of the non-solvent. Nonpolar cyclohexane was selected as the auxillary liquid, because sulfonated polysulfones exhibit little affinity for such alkanes [32,33].

### 2.2. Determination of $P_W$, $K_W$, and $D_W$

For water uptake measurements, hydrated BPS and BPSH films were dried in a vacuum oven at 100 °C for at least 48 h and were periodically weighed until a constant weight was obtained. While

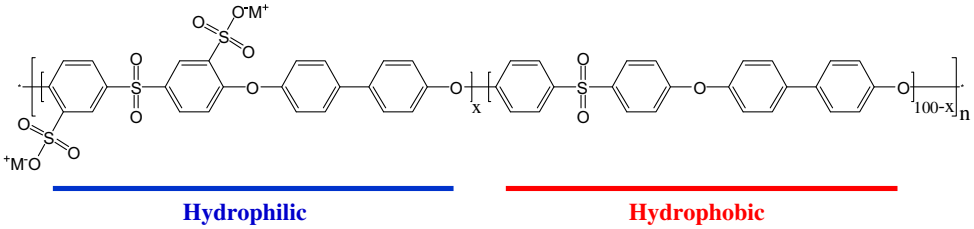


**Fig. 1.** Chemical structure of disulfonated poly(arylene ether sulfone) random copolymers: for BPS-X series, $M^+$ = metal ion, i.e. $K^+$; for BPSH-X series, $M^+$ = proton, i.e. $H^+$. X = mol% of SDCDPS, the disulfonated monomer, in sulfone monomers.

**Table 1**
Effect of water soaking time on water and salt permeability of BPS films.

| Material | Soaking time (h) | $P_W^H$ (L μm/(m$^2$ h bar)) | $P_S$ (cm$^2$/s) |
|---|---|---|---|
| BPS-20 | 1 | 0.033 ± 0.002 | (7.1 ± 0.3) × 10$^{-11}$ |
| | 96 | 0.040 ± 0.009 | (6.5 ± 0.6) × 10$^{-11}$ |
| BPS-40 | 1 | 0.62 ± 0.04 | (8.4 ± 1.0) × 10$^{-9}$ |
| | 96 | 0.57 ± 0.03 | (7.4 ± 0.2) × 10$^{-9}$ |

NOTE: For each data point, two samples were measured, and the average value is presented.

this procedure will presumably not remove the small amount of water which is tightly bound to the sulfonate groups, it does remove the vast majority of water from the sample. Then the films were immersed in deionized water at 25 °C and periodically weighed on an analytical balance until a constant water uptake was obtained. Tissue paper was used to wipe the film surface to remove water droplets on the film surface before weighing. The water uptake ($\omega_W$), i.e. the weight fraction of water in hydrated films, was calculated from the weight of the hydrated ($m_h$) and dried ($m_d$) films, respectively: [34]

$$\omega_W = \frac{m_h - m_d}{m_d} \tag{2}$$

Assuming ideal mixing behavior of water with BPS samples, the equilibrium volume fraction of water in the hydrated films ($\phi_W$) was estimated as follows:

$$\phi_W = \frac{(m_h - m_d)/\rho_W}{(m_h - m_d)/\rho_W + m_d/\rho_P} \tag{3}$$

where $\rho_W$ is the density of water (taken as 1.0 g/cm$^3$). The volume fraction of water can be used to calculate $K_W$, which is the water partition coefficient, or water solubility, in the polymer. $K_W$ is defined as the ratio of water concentration in the film, $C_W^m$, to that in the contiguous solution, $C_W$ [35,36]:

$$K_W = \frac{C_W^m}{C_W} \tag{4}$$

The units of $K_W$ are [g water/cm$^3$ swollen polymer]/[g water/cm$^3$ solution] [36]. For relatively dilute aqueous salt solutions (or pure water, of course), $C_W$ is equal to the density of pure water, $\rho_W$ [37]. $K_W$ is related to the volume fraction of water in the polymer, $\phi_W$, as follows:

$$K_W = \frac{\phi_W M_W}{C_W \overline{V_W}} \tag{5}$$

where $M_W$ is the molecular weight of water, and $\overline{V_W}$ is the partial molar volume of water in the polymer. $\overline{V_W}$ is set to be equal to the molar volume of water at ambient conditions, 18 cm$^3$/mol. With this assumption, and assuming that the water in contact with the polymer has the density of pure water, the water partition coefficient is equal to the volume fraction of water in the polymer:

$$K_W = \phi_W \tag{6}$$

Thus, water partition coefficient in the polymer and water volume fraction in the polymer are essentially equal, and we will use this approximation in the analysis of the data.

Pure water flux was measured using crossflow filtration in a system that has been previously described [30,31,38]. Three crossflow cells (CF042 Crossflow cell, Sterlitech Co., WA, USA) were connected in series, and the effective mass transfer area of each cell was 42 cm$^2$. The feed solution was deionized water; the feed flow rate was 1 gallon per minute (gpm) (i.e., 3.8 L/min); the applied feed pressure was 400 psig (27.2 atm); and the permeate pressure was atmospheric. Feed temperature was maintained at 25 °C using a refrigerated water bath (Neslab RTE 17, Thermo Scientific, Waltham, MA, USA). Water flux ($J_W$) was calculated as the volume of water ($\Delta V$) permeated at steady state through a film area ($A$) during a time period $\Delta t$:

$$J_W = \frac{\Delta V}{A \cdot \Delta t} \tag{7}$$

Hydraulic water permeability ($P_W^H$, L μm/(m$^2$ h bar)) was calculated from water flux, pressure difference across the film ($\Delta p$), and hydrated film thickness ($l$), as follows [37,39]:

$$P_W^H = \frac{J_W l}{\Delta p} \tag{8}$$

The thickness of the hydrated dense films studied was about 20–40 μm. The thicknesses of films were measured immediately before and after the crossflow measurements described above using a thickness gage (ABSOLUTE Digimatic Depth Gage Series 547, Mitutoyo, Japan) and were found not to have changed during the experiment. Moreover, the film thickness was expected to change negligibly during hydraulic permeation at the test conditions described above [40].

Based on the solution-diffusion model [35,37], a pressure difference applied across a film generates a water concentration gradient across the hydrated film, which drives the diffusion of water molecules. In situations where the Flory–Huggins model can be used to describe the effect of water activity on water uptake, which should be reasonable at least over the narrow range of water activities explored in these studies, the diffusive water permeability ($P_W^D$, cm$^2$/s) is related to hydraulic water permeability, which is measured in permeation tests, as follows: [35,40,41]:

$$P_W^D = K_W \cdot D_W = P_W^H \cdot \frac{RT}{\overline{V_W}}\left[(1 - K_W)^2(1 - 2\chi K_W)\right] \tag{9}$$

where $D_W$ is the average effective water diffusion coefficient across the film, $R$ is the ideal gas constant, $T$ is the absolute temperature of the measurement, and $\chi$ is the Flory–Huggins interaction parameter. In the Flory–Huggins theory, the chemical potential of the water, $a_W$, in a hydrated polymer is related to the concentration of water in the polymer as follows: [42,43]

$$\ln a_W = \ln K_W + (1 - K_W) + \chi(1 - K_W)^2 \tag{10}$$

Given $a_W$ (which is 1 for pure water) and the experimentally determined equilibrium volume fraction of water in each sample, an effective Flory–Huggins interaction parameter can be estimated, and the values obtained for the samples considered in this study are recorded in Table 2. Although there are no systematic studies that we are aware of to rigorously test the applicability of the Flory–Huggins model to systems such as those considered in this study, this approximation could be relaxed should more complete knowledge of the thermodynamics of interaction of water with such polymers be developed.

The concentration averaged, effective water diffusivity ($D_W$, cm$^2$/s) was estimated from known $P_W^D$ and $K_W$ values as follows: [40]

$$D_W = \frac{P_W^D}{K_W} \tag{11}$$

### 2.3. Determination of $P_S$, $K_S$, $D_S$ and $R$

Salt solubility ($K_S$) and diffusivity ($D_S$) were determined using kinetic desorption experiments [44–47]. Salt permeability ($P_S$) was then estimated as the product of salt diffusivity and solubility [37].

**Table 2**
Transport properties of disulfonated poly(arylene ether sulfone) films at 25 °C.

| Material | $R^a$ (%) | $K_W$ | $\chi^b$ | $K_S^c$ | $D_W^d \times 10^6$ (cm$^2$/s) | $D_S^c \times 10^7$ (cm$^2$/s) | $P_W^{H\,e}$ (L μm/(m$^2$ h bar)) | $P_W^D \times 10^7$ (cm$^2$/s) | $P_S^f \times 10^9$ (cm$^2$/s) |
|---|---|---|---|---|---|---|---|---|---|
| BPS-20 | 99.1 | 0.10 | 1.73 | 0.02 | 0.90 | 0.025 | 0.044 | 0.90 | 0.073 |
| BPS-30 | 97.8 | 0.19 | 1.30 | 0.03 | 1.4 | 0.38 | 0.22 | 2.8 | 1.5 |
| BPS-35 | 95.9 | 0.26 | 1.10 | 0.034 | 1.3 | 1.2 | 0.39 | 3.5 | 3.9 |
| BPS-40 | 93.5 | 0.29 | 1.05 | 0.043 | 1.7 | 3.0 | 0.65 | 5.0 | 8.7 |
| BPSH-20 | 98.5 | 0.20 | 1.26 | 0.021 | 1.1 | 0.082 | 0.19 | 2.3 | 0.77 |
| BPSH-30 | 92.3 | 0.32 | 0.99 | 0.036 | 1.8 | 5.5 | 0.89 | 5.7 | 22 |
| BPSH-35 | 88.4 | 0.40 | 0.88 | 0.057 | 2.1 | 9.8 | 2.1 | 8.7 | 103 |
| BPSH-40 | 84.5 | 0.48 | 0.79 | 0.081 | 2.3 | 20 | 4.4 | 11 | 226 |

[a] Measured at 25 °C using crossflow filtration (feed pressure = 27.2 atm (400 psig), flow rate = 1 gpm (3.8 L/min)), feed = 2000 ppm NaCl (0.034 M) aqueous solution.
[b] Calculated from water solubility using Equation 10.
[c] Measured via kinetic desorption experiments at 25 °C (initial concentration of NaCl in equilibration solution = 1 M).
[d] Calculated from water solubility and diffusive water permeability according to Equation 11.
[e] Measured at 25 °C using crossflow filtration (feed pressure = 27.2 atm (400 psig), flow rate = 1 gpm (3.8 L/min)), feed = deionized water.
[f] Measured at 25 °C using direct permeation cell (donor (upstream) concentration = 1 M NaCl; the downstream solution was initially deionized water).

An advantage of such experiments, relative to the direct permeation measurements described later, is that kinetic desorption experiments are insensitive to the presence of pinholes or film defects which could compromise a direct permeation measurement. As such, desorption experiments provide fundamental transport data without requiring the preparation of thin, defect-free samples required for direct permeation measurements.

Salt diffusivity ($D_S$) was determined from the rate of salt desorption into deionized water from films previously equilibrated with 60 mL of 1 M NaCl aqueous solution (#71394, Sigma–Aldrich, St. Louis, MO, USA) at 25 °C by soaking in that solution for at least 72 h. Following equilibration, the film was blotted with tissue paper to remove excess salt on the surface and subsequently placed in an extraction (i.e., desorption) bath containing 60 mL of initially deionized water that had been saturated with air to minimize any changes in solution conductivity with time due to absorption of atmospheric carbon dioxide. The extraction solution was well-stirred with a magnetic stir-bar to maintain uniform salt concentration throughout the extraction solution, and the extraction bath temperature was maintained at 25 °C. A conductivity probe (LR 325/01, WTW, Germany) with a nominal cell constant of 0.1 cm$^{-1}$ and a conductivity meter (InoLab Cond 730, WTW, Germany) were used to record the conductivity in the extraction bath as a function of time. The salt concentration was determined via a previously established calibration curve relating conductivity to salt concentration. The salt diffusivity was determined using a Fickian analysis for desorption from a plane sheet of film into a bath of finite volume [48]. The following equation was used to calculate the salt diffusivity from the desorption data [48]:

$$\frac{M_t}{M_\infty} = 1 - \frac{8}{\pi^2}\sum_{n=0}^{\infty}\frac{1}{(2n+1)^2}\exp\left[-(2n+1)^2\pi^2\frac{D_S t}{l^2}\right] \tag{12}$$

where $t$ is time, and $M_t$ is the mass of NaCl desorbed by the film up until time $t$. $M_\infty$ is the total amount of salt extracted from the film during the entire measurement, which corresponds to the amount of salt sorbed into the polymer when it had equilibrated with the 1 M NaCl soaking solution prior to the beginning of the desorption experiment. $D_S$ values were estimated by fitting the salt release kinetics data to a form of Equation 12 where the first 20 terms in the infinite series were retained for the data fitting.

The salt partition coefficient, or salt solubility, $K_S$, was determined by measuring the total amount of NaCl extracted during a kinetic desorption experiment (i.e., $M_\infty$) and calculated as the amount of salt extracted per unit volume of hydrated polymer, divided by the salt concentration in the solution with which the film was initially equilibrated (i.e., 1 M NaCl) [49]. The units of $K_s$ are (g NaCl/cm$^3$ hydrated film)/(g NaCl/cm$^3$ equilibration solution).

Salt permeability ($P_S$) was also directly measured at 25 °C using a dual chamber direct permeation cell (Side-Bi-Side Cells, PermeGear, Hellertown, PA, USA). A film was mounted between the two chambers of the glass cells. Each chamber had a volume of 35 mL. The active area available for mass transport, defined by the circular openings in the direct permeation cells, was 1.77 cm$^2$. The cells, with the film between them, were clamped tightly together. One chamber (the donor chamber) initially contained 1 M NaCl aqueous solution; the other chamber (the receptor chamber) was initially filled with deionized water. Stir-bars were placed in each chamber and stirred with a magnetic drive to make the solutions homogeneous. The concentration of salt in the receptor chamber was monitored as a function of time using the conductivity meter and probe described previously. At pseudo-steady state, the salt permeability was calculated using the following equation [49]:

$$\ln\left[1 - 2\frac{c_R(t)}{c_D(0)}\right]\left[-\frac{Vl}{2A}\right] = P_S t \tag{13}$$

where $c_R(t)$ is the receptor concentration at time $t$, $c_D(0)$ is the initial donor concentration, $V$ is the donor or receptor volume (35 mL in this case), and $A$ is the active film area (1.77 cm$^2$).

Salt rejection ($R$) was measured using crossflow filtration as described above. All of the experimental conditions were the same as those used for pure water permeability measurements, unless stated otherwise. The feed solution was an aqueous mixture containing 2000 mg/L NaCl (0.034 M), and the feed pH was adjusted to be between 6.5 and 7.5 using 0.1 M NaOH and HCl solutions (Fisher Scientific, Hampton, NH, USA). Feed and permeate salt conductivity values were measured using an Oakton 100 conductivity meter (Cole Parmer, Vernon-Hills, NJ, USA), and a calibration curve was used to calculate salt concentration from solution conductivity. The salt rejection was calculated as follows:

$$R = 1 - \frac{C_P}{C_F} \tag{14}$$

where $C_P$ and $C_F$ are the concentrations of salt in the permeate and feed solutions, respectively. Because the samples being characterized were thick, dense films, resulting in low fluxes of water and salt, concentration polarization did not influence these measurements, so no correction for it was needed. Hydraulic water permeability coefficients were also calculated from crossflow filtration measurements with a feed of 2000 ppm NaCl aqueous solution. To account for the influence of osmotic pressure difference across the film ($\Delta\pi$) on the water permeability, the following equation was used instead of Equation 8:

$$P_W^H = \frac{J_W l}{(\Delta p - \Delta \pi)} \quad (15)$$

In this case, the ideal solution expression for the osmotic pressure difference (i.e. $\Delta\pi = RT(C_F - C_P)$ was used to calculate $\Delta\pi$. The hydraulic water permeability coefficients of BPS-35 ($P_W^H$ = 0.38 L μm/(m$^2$ h bar)) and BPSH-35 ($P_W^H$ = 2.0 L μm/(m$^2$ h bar)) were measured using this protocol. Within the uncertainty of the measurements, the hydraulic water permeability coefficients measured with a feed containing 2000 ppm NaCl aqueous solution is equal to that measured with a feed of deionized water as shown in Table 2 ($P_W^H$ (BPS-35) = 0.39 L μm/(m$^2$ h bar) and ($P_W^H$ (BPSH-35) = 2.1 L μm/(m$^2$ h bar)).

## 3. Results and discussion

As shown in Fig. 1, BPS copolymers can be prepared with various levels of sulfonation and in both acid and salt forms. As will be shown below, transport properties of these copolymers vary significantly with both sulfonation level and ion form (i.e., acid or salt form). Generally, as sulfonation level increases, water permeability increases and salt rejection decreases, and acid form materials have higher water permeability and lower salt rejection than their salt form analogs [28]. In this study, the sulfonation level was kept below 50% to maintain significant levels of salt rejection and to keep the polymers from becoming water-soluble.

### 3.1. Water uptake

Fig. 2 presents the water uptake in volume fraction (mL water/mL hydrated polymer), of BPS copolymers with various degrees of sulfonation in both acid and salt forms. The water sorption increases as the concentration of hydrophilic SDCDPS comonomer increases. The initially acid form films have higher water uptake than films prepared from samples that were initially in the salt form. The water uptake increases non-linearly with sulfonation level, increasing more rapidly at higher levels of sulfonation. Tapping mode phase image atomic force microscopy (AFM) studies reveal two regions in the microstructure of BPS copolymers: ionic domains, where the ions are not evenly distributed but aggregate to form hydrophilic ion clusters, and a matrix of non-ionic hydrophobic regions [21,50]. At low sulfonation level, the hydrophilic ion clusters form isolated ionic domains, and as the amount of disulfonated groups increases, the size of the isolated ion clusters grows. When the level of sulfonation reaches a sufficiently high level, e.g. 50%, the ionic domains undergo a significant change, becoming continuous and forming large channels of an ionic rich phase. Once the continuous hydrophilic phase forms, the water uptake increases dramatically [21]. Thus, as the sulfonation level approaches this critical point, where the ionic domains become continuous and form large, ionic-containing regions in the sample, water uptake becomes more sensitive to sulfonation level.

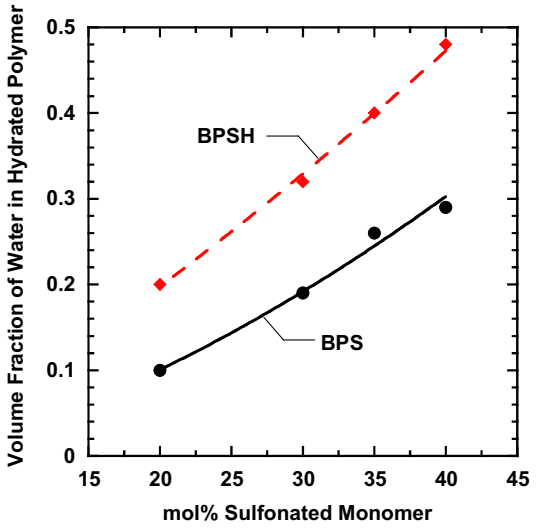


**Fig. 2.** Effect of sulfonated monomer content on water uptake of BPS and BPSH films at 25 °C.

### 3.2. Water permeability and diffusivity

Fig. 3 shows the effect of feed pressure on water flux for two representative polymer samples considered in this study. In both the acid and salt forms, the pure water flux is linearly related to feed pressure over the pressure range considered. The results shown in Fig. 3 are representative of results obtained for all other samples considered, which are not shown for brevity. Data such as those in Fig. 3 were used, along with Equation 8, to calculate hydraulic water permeability coefficients.

Fig. 4(a) presents the hydraulic water permeability coefficients of BPS and BPSH films measured in crossflow filtration. Generally, hydraulic water permeability increases systematically with increasing concentration of the hydrophilic sulfonated monomer, and the hydraulic water permeability of acid form samples is higher than that of salt form films having the same SDCDPS content. Hydraulic water permeability is also somewhat more sensitive to sulfonated monomer content in the acid form materials than in the salt form films. For example, the hydraulic water permeability of the 40 mol % sulfonated sample is 14 times higher than that of the 20 mol % sample in the salt form and 22 times higher in the acid form samples.

Water solubility, $K_W$, and effective water diffusivity, $D_W$, in the hydrated polymers were calculated using Equations 6 and 11. These values are reported in Table 2. Water solubility is determined by water sorption and film density, as discussed earlier, and it, like water uptake, increases with increasing sulfonation level.

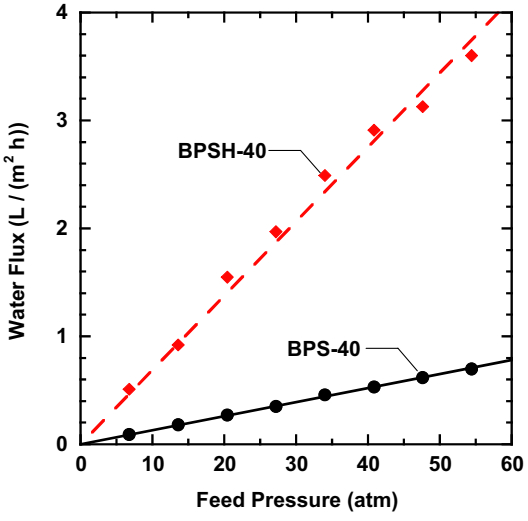


**Fig. 3.** Effect of feed pressure on water flux of BPS and BPSH dense films. The samples presented in this figure are BPS-40 (thickness ≈ 45 μm) and BPSH-40 (thickness ≈ 70 μm). Test conditions: dead-end filtration, temperature = 25°C, feed = deionized water, downstream pressure = 1 atm.

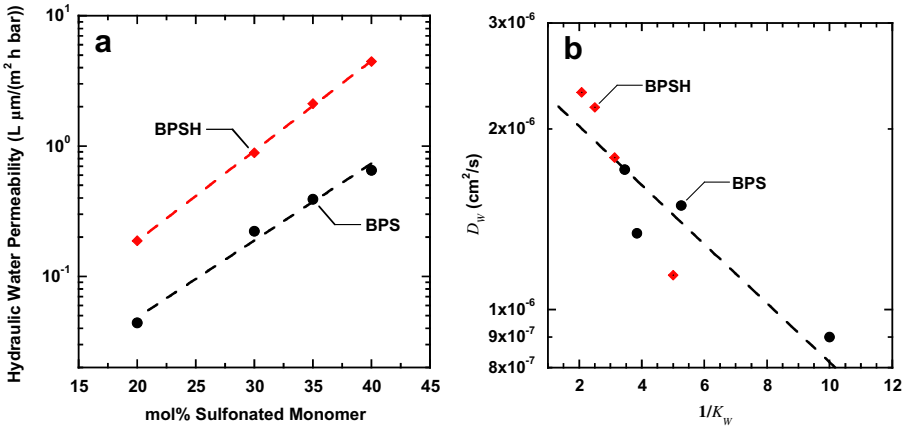


**Fig. 4.** (a) Effect of sulfonated monomer content on pure water permeability of BPS and BPSH dense films at 25 °C; (b) Water diffusivity, $D_W$, as a function of $1/K_W$, which is the reciprocal of water volume fraction in hydrated BPS and BPSH films. Test conditions: crossflow filtration, feed pressure = 400 psig (27.2 atm), feed flow rate = 1 gpm.

The effective water diffusion coefficients in these samples are presented as a function of $1/K_W$ in Fig. 4(b). The motivation for presenting the data as the logarithm of the diffusion coefficient versus $1/K_W$ comes from Yasuda's studies suggesting that in hydrated polymers, free volume theory should govern the diffusion of small penetrant molecules, such as water and salt, and that free volume of the polymer/water mixture should be proportional to the volume fraction of water in the polymer (i.e., $K_W$) [49] If this is the case, then the logarithm of the diffusion coefficient should be a linear function of $1/K_W$. The line through the data represents a fit of Yasuda's model to the data, and, to a first approximation, the water diffusion coefficients follow the trend expected from Yasuda's model [49].

### 3.3. Salt permeability and salt rejection

Salt flux, $J_S$, is related to salt permeability as follows [35,37,39]

$$J_S = \frac{P_S}{l} \cdot \Delta C_S \tag{16}$$

where $\Delta C_S$ is the salt concentration difference in the solutions on the feed and permeate sides of the film. In this regard, Fig. 5(a) presents the influence of sulfonated monomer content on NaCl permeability measured in a direct permeation cell [28]. Consistent with the water permeation results presented in Fig. 4, the salt permeability increases monotonically with increasing sulfonated monomer content, and the salt permeability is higher in acid form samples than in salt form samples.

The effect of feed NaCl concentration on the NaCl permeability of BPS-32 was also investigated, and the results are shown in Fig. 5 (b). Generally, the NaCl permeability increases as feed NaCl concentration increases. In highly charged polymers, such as the hydrated BPS and BPSH films, the fixed sulfonate anion groups tend to repel $Cl^-$ ions. As the concentration of salt increases in the external solution, the salt concentration in the polymer increases, so the fixed anion groups in the polymer matrix become more shielded from interacting with surrounding ions, resulting in an increase in NaCl permeability at higher salt concentrations. In other highly charged polymers, it is not unusual for salt permeability to increase as external salt solution concentration increases [51].

The results presented in Fig. 5 were derived from direct permeation cell measurements, so they were conducted with atmospheric pressure on both sides of the sample. Salt rejection coefficients reported in Fig. 6 were measured from both dead-end filtration experiments (●,○) [28] and crossflow filtration experiments (▲,△). Salt rejection of both the acid and salt form films decreases as sulfonation level increases. At lower sulfonation levels, the salt rejection of the free acid and salt form films are similar to one another, but rejection decreases more with increasing sulfonation level in the free acid form films than in the salt form films. This behavior is qualitatively similar to the influence of sulfonation level on water permeability (cf., Fig. 4). Salt rejection values measured via crossflow filtration are slightly higher than those from dead-end filtration measurements reported earlier [28] due to the elimination of salt concentration polarization in the crossflow experiments, which is difficult to avoid in dead-end filtration measurements of salt transport.

Salt rejection is related to water and salt permeability, as well as operational variables such as pressure, salt concentration, and temperature as follows [37,39]:

$$R = \frac{\frac{P_W^H}{P_S}(\Delta p - \Delta\pi)}{1 + \frac{P_W^H}{P_S}(\Delta p - \Delta\pi)} \times 100\% \tag{17}$$

Using this result and the water and salt permeability coefficients reported in Table 2, one may calculate the rejection, based on direct permeation cell measurements of salt permeability and crossflow measurements of pure water permeability. A comparison of the calculated rejection coefficients (■, □) with those measured during crossflow filtration and dead-end filtration of a 2000 ppm NaCl solution is shown in Fig. 6. There are significant differences between the calculated rejection coefficients and the measured values. We ascribe these differences to the fact that the crossflow and direct permeation measurements were run at very different salt concentrations. For example, in the crossflow measurements, the salt rejection was determined with a feed concentration of 2000 ppm NaCl, which corresponds to 0.034 M NaCl. In the direct permeation measurements, the feed concentration of NaCl was 1 M. Based upon the information in Fig. 5(b), the NaCl permeability coefficient increased approximately five times as the feed concentration of NaCl aqueous solution increased from 0.034 M to 1 M. Therefore, it is not unreasonable that the calculated rejection coefficients in Fig. 6 are lower than the directly measured values.

### 3.4. Salt solubility and diffusivity derived from kinetic desorption measurement

An example of results from a NaCl kinetic desorption experiment is presented in Fig. 7. The salt diffusivity was obtained by

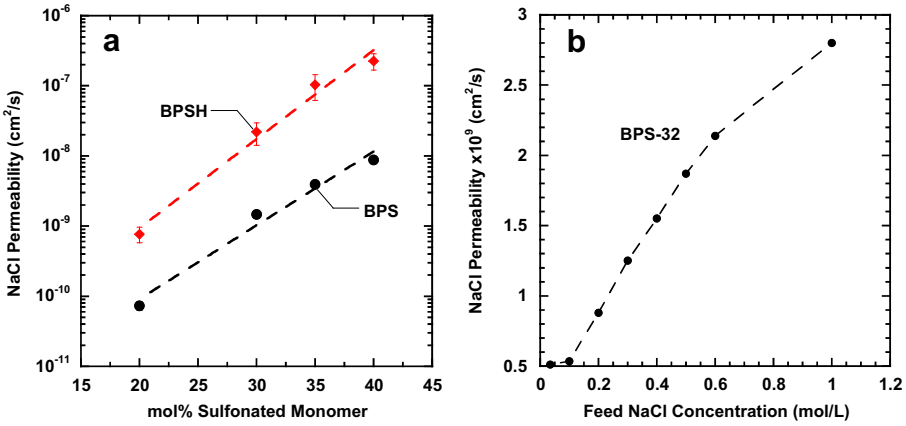


**Fig. 5.** Effect of a) sulfonated monomer content on salt permeability of BPS and BPSH dense films and b) donor concentration on salt permeability of BPS-32 at 25 °C. Test conditions: direct permeation cell, upstream (donor) concentration = 1 M NaCl (for Fig. 5(a)), downstream (receptor) initially contains deionized water at ambient pressure [28].

fitting the entire desorption curve using the solution from Crank [48]. Based upon the results in Fig. 7, the desorption kinetics are more rapid in the acid form film (BPSH-40) than in the salt form film (BPS-40), indicating that the salt diffusivity was higher in the acid form sample.

Fig. 8 presents salt solubility and diffusivity as a function of sulfonation level. Acid form samples have higher diffusivity than their salt form analogs at the same sulfonation level. The salt solubility is similar in acid and salt form samples having the lowest sulfonation degree (i.e., 20%), but at higher degrees of sulfonation, the acid form material has higher NaCl solubility than that of its analogous salt form material.

Based upon Yasuda et al.'s studies of NaCl sorption and transport in hydrated polymers, salt solubility and diffusivity are expected to increase as water uptake increases [49]. Yasuda et al. used free volume theory to describe the influence of water content on small molecule diffusivity in hydrated polymers. According to free volume theory, the connection between free volume and diffusivity is given by: [52]

$$D = A \cdot \exp\left[-\frac{\gamma v^*}{v_f}\right] \tag{18}$$

where $A$ is a constant, $\gamma$ is a parameter introduced to avoid double counting the free volume elements, $v_f$ is the free volume in the sample under study, and $v^*$ is a characteristic volume required to accommodate the small molecule penetrant diffusing through the polymer. Yasuda et al. suggested that the free volume of a hydrated polymer could be expressed as the free volume of the polymer plus the free volume of the water in the polymer: [49]

$$v_f = K_W \cdot v_{f,H_2O} + (1 - K_W) v_{f,polym} \tag{19}$$

where $v_{f,H_2O}$ and $v_{f,polym}$ are the free volumes of bulk water and dry polymer, respectively. Yasuda et al. proposed that salt would permeate through the polymer matrix at a very slow rate, so that appreciable salt diffusion would only occur when the polymer was

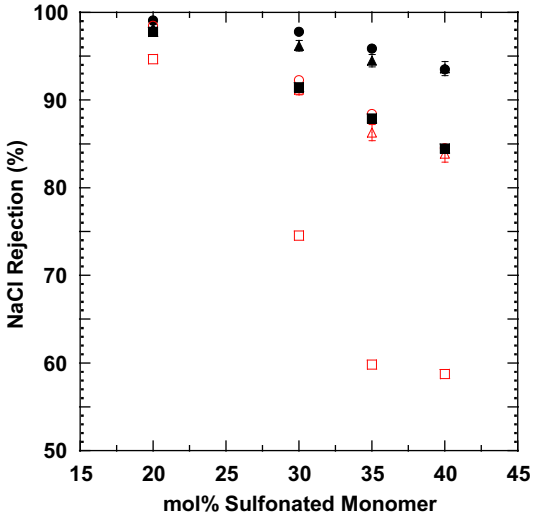


**Fig. 6.** Effect of sulfonated monomer content on salt rejection of dense films of disulfonated copolymers at 25 °C. Filled symbols are BPS films, and open symbols are BPSH films. Test conditions (●,○): crossflow filtration, feed pressure = 400 psig (27.2 atm), feed flow rate = 1 gpm, feed composition: 2000 ppm NaCl aqueous solution, pH = 6.5–7.5; Test conditions (▲,△) [28]: dead-end filtration, feed pressure = 400 psig (27.2 atm), feed composition: 2000 ppm NaCl aqueous solution, pH = 6.5–7.5, stirring speed = 300 rpm; Estimation of rejection from Equation 17 (■,□): $P_S$ was measured in direct permeation cell with a feed of 1 M NaCl aqueous solution, and $P_W$ was obtained from pure water flux measurement. To calculate rejection from known $P_S$ and $P_W$ values, $\Delta p$ was set to 400 psig (27.2 atm) and $\Delta\pi$ was calculated assuming the NaCl concentration difference was 2000 ppm to be consistent with the measurement conditions of the crossflow studies.

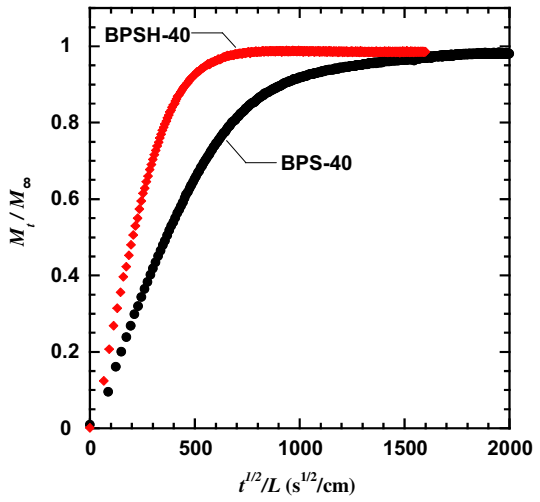


**Fig. 7.** Kinetic salt desorption of BPS-40 and BPSH-40 at 25 °C. The films were equilibrated in 1 M NaCl aqueous solution at 25 °C, and the kinetic desorption data were measured when the films were placed in deionized water at 25 °C.

hydrated. Consequently, the free volume important for salt transport through a hydrated polymer is that added to the polymer by the water. As a result, Yasuda et al. simplified Equation 19 as follows:

$$v_f \cong K_W \cdot v_{f,H_2O} \tag{20}$$

Yasuda et al. proposed the following expression relating the water uptake in the sample, $K_W$, to salt diffusivity, $D_S$: [49]

$$\ln D_S = \ln D_0 - B\left(\frac{1}{K_W} - 1\right) \tag{21}$$

where $D_0$ is the diffusivity of NaCl in pure water at the temperature of the experiment, taken as $1.47\times10^{-5}$ cm$^2$/s at 25 °C [49], and $B$ is a proportionality constant related to the characteristic volume, $v^*$, and $v_{f,H_2O}$. Based on this model, a plot of log $D_S$ versus $1/K_W$ is expected to be linear and pass through the dilute solution diffusivity of NaCl in water (i.e., at $1/K_W = 1$). Fig. 9(a) presents the NaCl diffusivity data obtained in this study along with data from Yasuda's study plotted as suggested by Equation 21. The data follow Yasuda's model to a reasonable extent and illustrate the close connection between water uptake and salt diffusivity in a wide variety of polymers.

Water diffusivity and salt diffusivity of BPS and BPSH films are presented together in Fig. 9(b) as a function of $1/K_W$. To a first approximation, both water and salt permeability vary exponentially with $1/K_W$, showing reasonable coherence with Yasuda's free volume theory. Moreover, the NaCl permeability of BPS and BPSH films is more sensitive than that of the water permeability to changes in water solubility, $K_W$, due to larger size of hydrated $Na^+$ and $Cl^-$ ions relative to the size of a water molecule, which is also consistent with free volume theory (i.e., smaller penetrants should show a weaker dependence of diffusion coefficients on free volume (i.e., water content, in this case) than larger penetrants). For example, the water diffusion coefficients decrease by a factor of 3 in Fig. 9(b), as water content goes from its highest to lowest value, while the salt diffusion coefficients decrease by a factor of 800.

Fig. 10 presents salt solubility as a function of water uptake for BPS and BPSH polymers as well as a selection of literature data for comparison. The salt solubility coefficient characterizes the concentration of NaCl in a hydrated film relative to the salt concentration in the surrounding solution. Yasuda proposed that, in the simplest scenario, the salt solubility in a hydrated polymer would simply be equal to the water solubility: $K_S = K_W$ [49]. That is, the polymer would sorb salt in proportion to the amount of water sorbed by the polymer. Clearly, this model is a highly approximate and simplistic approach to what may well be a complex interplay between the salt ions, ionic and non-ionic moieties in the polymer backbone, and the water present in the swollen sample. For example, Yasuda found cases where the salt solubility was significantly less than the water uptake [49]. For some hydrated polymers (i.e., HPMA-GMA and HPMA-MMA from Yasuda's studies [49]), the salt solubility remains close to water solubility even when the swollen film had low water solubility (cf., Fig. 10). Conversely, other polymers (HEMA, CA, BPS, and BPSH) show lower salt solubility than water solubility in Fig. 10, suggesting that, in these cases, the polymers could reject ions based, in part, on the thermodynamic partitioning of ions in the polymer.

Salt permeability can also be estimated from kinetic desorption data by multiplying the salt solubility and diffusivity together as follows [37]:

$$P_S = D_S \cdot K_S \tag{22}$$

Fig. 11 presents a comparison of permeability coefficients measured in direct permeation experiments [28], those calculated as the product of salt solubility and diffusivity determined in kinetic desorption experiments, and those calculated from salt rejection and water permeability based on Equation 17. Samples studied in direct permeation and kinetic desorption experiments were studied using a 1 M NaCl solution as the feed solution (direct permeation) or soaking solution (kinetic desorption), whereas the crossflow experiments were performed at much lower salt concentration, 2000 ppm (i.e., 0.034 M). The salt permeabilities estimated from the kinetic desorption studies and measured in direct permeation cell experiments are very similar to one another, providing a good check on the applicability of the solution-diffusion model (i.e., Equation 22). The crossflow filtration data yielded systematically lower salt permeability coefficients than other methods due to the lower salt concentration in the feed, which is consistent with the results shown in Fig. 5(b).

As shown in Fig. 12, for the highly hydrated, essentially uncharged hydrogels considered in Yasuda's study, the salt permeability coefficients decrease exponentially as $1/K_W$ increases. In Yasuda's materials, the dominant contribution of water content on salt permeability is its influence on salt diffusion coefficients, which decreases exponentially as $1/K_W$ increases. In fact, the Yasuda salt permeability data extrapolate to a value of the salt diffusion coefficient in water in a hypothetical membrane composed entirely of water (i.e., $1/K_W = 1$). This is a reasonable trend since, in such a hypothetical membrane, the salt partition

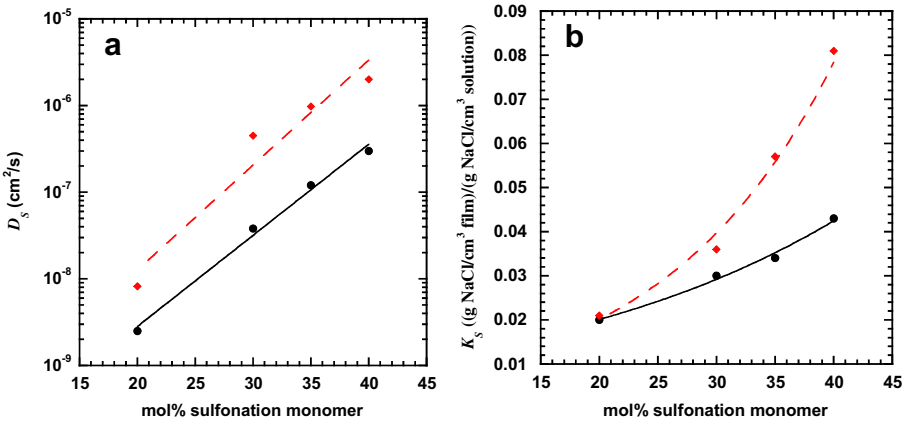


**Fig. 8.** Effect of sulfonated monomer content on a) NaCl diffusivity and b) NaCl solubility in BPS and BPSH films at 25 °C. These data are from kinetic desorption experiments, such as those presented in Fig. 7, with samples initially equilibrated in 1 M NaCl aqueous solution.

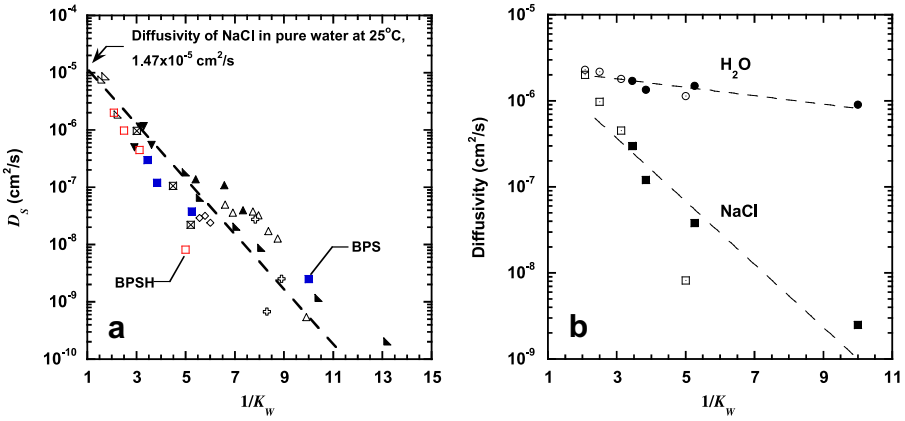


**Fig. 9.** a) NaCl diffusivity, $D_S$, as a function of $1/K_W$, which is the reciprocal of the pure water volume fraction in hydrated polymer. The dashed line represents a fit of all of the data points to Equation 21, where the fit is forced through the point (at $1/K_W = 1$) representing the diffusivity of NaCl in water; b) Water and NaCl diffusivity of BPS and BPSH as a function of $1/K_W$. For the BPS and BPSH data, $D_S$ was determined from kinetic desorption studies following equilibration in an aqueous salt solution which contained 1.0 M NaCl, and $D_W$ was calculated from pure water permeability and solubility according to Equation 11. Experimental temperature = 25 °C. BPS (■,●); BPSH (□,○); HPMA-GMA (◺) = hydroxypropyl methacrylate - glycerol methacrylate copolymer [49]; HEMA (▼) = hydroxyethyl methacrylate polymer [49]; MMA-GMA (◣) = methyl methacrylate - glycerol methacrylate copolymer [49]; HEMA-MMA (▲) = hydroxyethyl methacrylate - methyl methacrylate copolymer [49]; HPMA-MMA (△) = hydroxypropyl methacrylate - methyl methacrylate copolymer [49]; HPMA-GDMA (◆) = hydroxypropyl methacrylate - glycidyl methacrylate copolymer [49]; CA (✠) = cellulose acetate [49]; and HEMA2 (⊠) = hydroxyethyl methacrylate [53].

coefficient should be unity and, therefore, the salt permeability coefficient should be equal to the salt diffusion coefficient in water.

Salt permeability data in the BPS and BPSH materials are also presented in Fig. 12. They all lie below the data for Yasuda's hydrogels and do not follow a simple linear relation with $1/K_W$. Since the salt diffusion coefficients in the BPS and BPSH materials largely follow the same relation with water uptake as Yasuda's materials (cf., Fig. 9(a)), the difference is due to the fact that the BPS and BPSH materials have significantly lower salt partition coefficients than the Yasuda hydrogels (cf., Fig. 10).

### 3.5. Water/salt selectivity

The separation performance of a polymeric film for desalination is often described in terms of water flux and salt rejection. However, since salt rejection is a function of applied pressure difference and salt concentration, it does not characterize the intrinsic separation properties of a polymeric film. Moreover, water flux depends on the membrane thickness and applied pressure difference, so it also depends on variables other than the inherent properties of the material. This thickness, pressure and concentration dependence makes it difficult to compare inherent separation properties of polymeric films because films may be prepared at a variety of thicknesses and tested under a variety of conditions. Consequently, the water and salt permeability coefficients and, to characterize inherent separation properties of a polymer, the ratio of water to salt permeability coefficients of polymeric films, provide metrics for evaluating material performance that are less sensitive to the details of particular experiments than flux and rejection [54].

According to the solution-diffusion theory, diffusive water permeability is defined as in Equation 9, and salt permeability is shown in Equation 22. Then, the ideal water/salt selectivity, $\alpha_{W/S}$, is defined as the ratio of water to salt permeability:

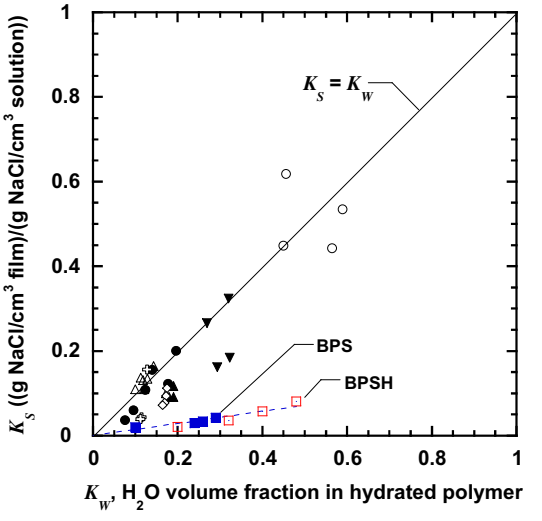


**Fig. 10.** Influence of water uptake, $K_W$, on NaCl solubility, $K_S$. For the BPS and BPSH data, $K_S$ was determined from kinetic desorption studies following equilibration in an aqueous salt solution at 25 °C which contained 1 M NaCl, and $K_W$ was measured in pure water. Experimental temperature = 25 °C (◺) = HPMA-GMA [49]; (▼) = HEMA [49]; (◣) = MMA-GMA [49]; (▲) = HEMA-MMA [49]; (△) = HPMA-MMA [49]; (◆) = HPMA-GDMA [49]; (✠) = cellulose acetate [49].

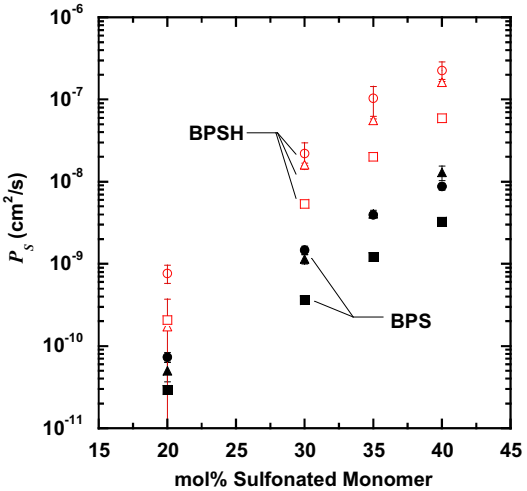


**Fig. 11.** Effect of sulfonated monomer content on salt permeability of BPS dense films measured via different methods at 25 °C. (●,○): direct permeation test, feed composition: 1 M NaCl aqueous solution [28]; (▲,△): kinetic desorption test, with samples initially equilibrated in 1 M NaCl aqueous solution; (■,□): crossflow filtration, feed = 2000 ppm (0.034 M) NaCl aqueous solution.

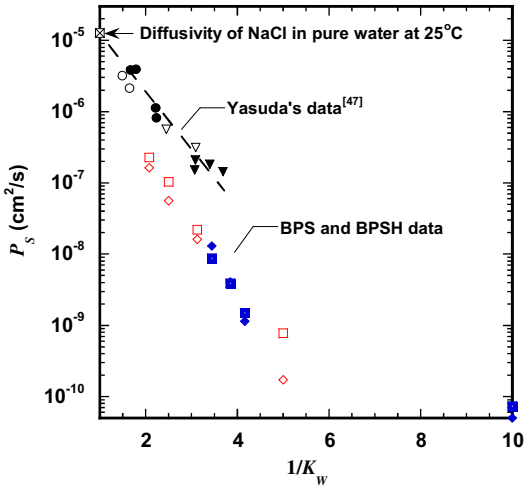


**Fig. 12.** NaCl permeability, $P_S$, as a function of $1/K_W$ at 25 °C. (○) = HPMA-GMA (direct permeation) [49]; (▽) = HEMA (direct permeation) [49]; (●) = HPMA-GMA ($P_S = K_S \times D_S$) [49]; (▼) = HEMA ($P_S = K_S \times D_S$) [49]; (■) = BPS (direct permeation, feed concentration = 1 M NaCl); (□) = BPSH (direct permeation: feed concentration = 1 M NaCl); (◆) = BPS (kinetic desorption: salt permeability was calculated from $P_S = K_S \times D_S$, and samples were initially equilibrated in 1 M NaCl aqueous solution); (◇) = BPSH (kinetic desorption: samples were initially equilibrated in 1 M NaCl aqueous solution).

$$\alpha_{W/S} = \frac{P_W^D}{P_S} \tag{23}$$

Substituting into Equation 17 yields

$$R = 1 - \frac{1}{1 + \alpha_{W/S}\dfrac{\overline{V_W}}{RT}\cdot\dfrac{(\Delta p - \Delta\pi)}{(1-K_W)^2(1-2\chi K_W)}} \tag{24}$$

The selectivity ($\alpha_{W/S}$) characterizes the intrinsic ability of a polymeric film to separate water and salt. In contrast, salt rejection is determined by the selectivity as well as details that would be particular to the experiment being used to make the measurement, such as the applied pressure difference and osmotic pressure difference (cf., Equation 24). Of course, if the salt and/or water permeability depend on salt concentration, then the selectivity may also depend on salt concentration.

Given that water and salt permeability depend on solubility and diffusivity (as shown in Equation 22), both water and salt solubility and diffusivity contribute to determining the water/salt separation properties of a polymer as follows

$$\alpha_{W/S} = \frac{P_W^D}{P_S} = \frac{K_W}{K_S} \times \frac{D_W}{D_S} \tag{25}$$

Thus, the water/salt permeability selectivity depends on the water/salt solubility selectivity and diffusivity selectivity.

Fig. 13 presents the water/salt diffusivity selectivity as a function of water diffusivity for BPS, BPSH and a variety of polymers from the literature. Polyamide-type polymer films exhibit high diffusivity selectivity, and highly water-swollen neutral hydrogel polymers, such as crosslinked poly(ethylene oxide) [55], show low diffusivity selectivity. The disulfonated BPS and BPSH films display a wide range of diffusivity selectivities depending on the sulfonation level and the sulfonate form (i.e., free acid form or salt form). In general, polymers with higher concentrations of sulfonic acid groups and those in the free acid form display higher water diffusivity and lower water/salt diffusivity selectivity values, and there is a general tradeoff between these two variables. The dashed line is from a recent paper and represents the best combinations of water diffusivity and water/salt diffusion selectivity currently known (i.e., the so-called upper bound for diffusion and diffusion selectivity) [54]. There are no materials today to the right of the dashed line.

The water/salt solubility selectivity values of BPS, BPSH, and a variety of polymers from the literature are presented in Fig. 14 as a function of water uptake. Interestingly, there appears to also be a tradeoff observed: polymers having high water solubility tend to have high NaCl solubility, so they have low water/NaCl solubility selectivity. The dashed line in the figure is from the literature [54].

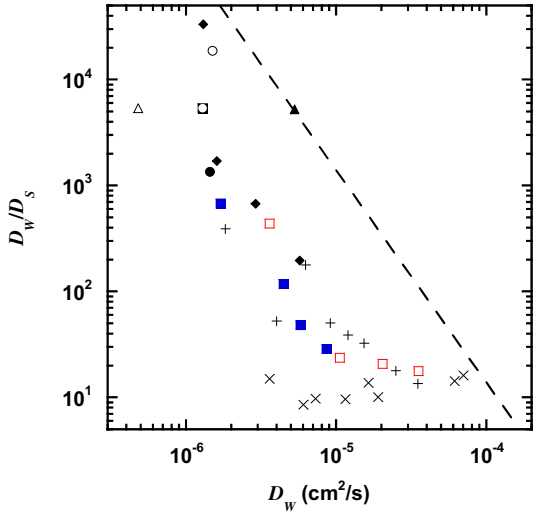


**Fig. 13.** Water/NaCl diffusivity selectivity as a function of water diffusivity in dense films: PI (△) = polyimide [56], PA1 (●) = aromatic polyamide [56], PBP (▲) = polybenzimidazopyrrolone [56], PAH (◘) = polyamide-hydrazide [56], CA (◆) = cellulose acetate [39], PA2 (○) = aromatic polyamide [57], PEG (×) = poly (ethylene glycol) [55], BPS (+) = disulfonated polysulfones reported previously [12,54], and BPS (■) and BPSH (□) = disulfonated polysulfones from this study. For BPS and BPSH data, $D_W$ were calculated using Equations 9 and 11 assuming $(1-K_W)^2(1-2\chi K_W) = 1$. The dashed line is the upper bound [54].

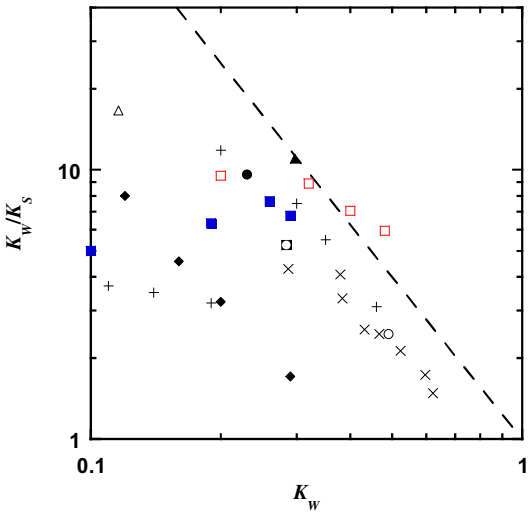


**Fig. 14.** Water/NaCl solubility selectivity as a function of water partition coefficient in dense films: PI (△) = polyimide [56], PA1 (●) = aromatic polyamide [56], PBP (▲) = polybenzimidazopyrrolone [56], PAH (◘) = polyamide-hydrazide [56], CA (◆) = cellulose acetate [39], PA2 (○) = aromatic polyamide [57], PEG (×) = poly (ethylene glycol) [55], BPS (+) = disulfonated polysulfones reported previously [12,54], and BPS (■) and BPSH (□) = disulfonated polysulfones from this study. The dashed line is the upper bound [54].

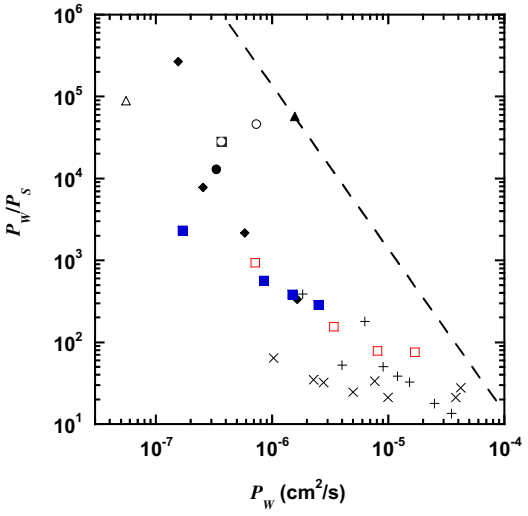


**Fig. 15.** Water/NaCl permeability selectivity as a function of diffusive water permeability in dense films: PI (△) = polyimide [56], PA1 (●) = aromatic polyamide [56], PBP (▲) = polybenzimidazopyrrolone [56], PAH (◘) = polyamide-hydrazide [56], CA (◆) = cellulose acetate [39], PA2 (○) = aromatic polyamide [57], PEG (×) = poly (ethylene glycol) [55], BPS (+) = disulfonated polysulfones reported previously [12,54], and BPS (■) and BPSH (□) = disulfonated polysulfones from this study. For BPS and BPSH data, $P_W$ were calculated using Equation 9 assuming $(1 - K_W)^2(1 - 2\chi K_W) = 1$. The dashed line is the upper bound [54].

In general, differences in solubility selectivity are smaller than those in diffusivity selectivity for the same family of polymers. For the BPS and BPSH materials, samples with higher concentrations of sulfonate salt groups and those in the free acid form display higher water solubility coefficients and lower water/salt solubility selectivity values.

Finally, Fig. 15 presents a correlation between water permeability and water/salt permeability selectivity. This plot resembles the well-known permeability selectivity tradeoff plot for films used in gas separations [58–60]. Apparently, there is a tradeoff between water permeability and water/salt permeability selectivity, and the line in this paper is from a recent article discussing the tradeoff in more detail [54]. In the BPS and BPSH polymers, samples with higher concentrations of sulfonate salt groups and those in the free acid form display higher water permeability coefficients and lower water/salt permeability selectivity values.

## 4. Conclusions

A series of disulfonated poly(arylene ether sulfone) random copolymers was prepared with a range of sulfonation levels in both salt and acid forms. The desalination properties of these polymers were characterized. The sulfonation level and ionic form of the polymers strongly influence water uptake in the polymers, with polymers in the acid form and those having higher concentrations of sulfonic acid groups having higher water uptake. The water diffusion and permeation properties, as well as salt solubility, diffusivity and permeability were well correlated with water uptake in these materials; samples with higher water uptake had higher water diffusivity and permeability as well as higher salt solubility, diffusivity and permeability. There appear to be tradeoffs between water solubility, diffusivity, and permeability with water/salt solubility, diffusivity and permeability selectivity. Samples with higher water solubility, diffusivity and permeability generally had lower values of water/salt solubility, diffusivity and permeability selectivity.

## Acknowledgements

This work was supported by the National Science Foundation (NSF)/Partnerships for Innovation (PFI) Program (Grant # IIP-0650277 and IIP-0917971) and CBET-0932781/0931761. Additionally, this work was supported by the NSF Center for Layered Polymeric Systems (Grant DMR-0423914). HBP acknowledges support from the World Class University (WCU) Program of the Ministry of Education, Science and Technology (MEST) and also support from the Industrial Source Technology Development Program (10035373) of the MKE of Korea.

## References

[1] Lonsdale HK. Journal of Membrane Science 1982;10(2–3):81–181.
[2] Petersen RJ. Journal of Membrane Science 1993;83(1):81–150.
[3] Cadotte JE. Interfacially synthesized reverse osmosis membrane. U.S. patent 4,277,344, 1981.
[4] Geise GM, Lee H-S, Miller DJ, Freeman BD, McGrath JE, Paul DR. Journal of Polymer Science Part B: Polymer Physics 2010;48(15):1685–718.
[5] Greenlee LF, Lawler DF, Freeman BD, Marrot B, Moulin P. Water Research 2009;43(9):2317–48.
[6] Reese ET, Mandels M. Cellulose and cellulose derivatives. NY: Wiley Interscience; 1971.
[7] Knoell T. Ultrapure Water 2006;23:24–31.
[8] Avlonitis S, Hanbury WT, Hodgkiess T. Desalination 1992;85(3):321–34.
[9] Nunes SP, Peinemann KV. Membrane technology in the chemical industry. Weinheim: Wiley-VCH; 2006.
[10] Robeson LM, Farnham AG, McGrath JE. Dynamic mechanical characteristics of polysulfone and other polyarylethers. In: Meier DJ, editor. Molecular basis for transitions and relaxations, vol. 4. Midland Macromolecular Institute Monographs; 1978. p. 405–26.
[11] Glater J, Hong SK, Elimelech M. Desalination 1994;95(3):325–45.
[12] Park HB, Freeman BD, Zhang ZB, Sankir M, McGrath JE. Angewandte Chemie, International Edition 2008;47(32):6019–24.
[13] Noshay A, Robeson LM. Journal of Applied Polymer Science 1976;20 (7):1885–903.
[14] Brousse C, Chapurlat R, Quentin JP. Desalination 1976;18(2):137–53.
[15] Allegrezza AE, Parekh BS, Parise PL, Swiniarski EJ, White JL. Desalination 1987;64:285–304.
[16] Kimura SG. Industrial & Engineering Chemistry Research 1971;10:335–9.
[17] Friedrich C, Driancourt A, Noël C, Monnerie L. Desalination 1981;36(1):39–62.
[18] Quentin JP. Sulfonated polyarylethersulfones. U.S. patent 3,709,841, 1973.
[19] Graefe AF, Saitonstall Jr. CW, Schell WJ. Process for the preparation of a stable salt form of a sulfonated polyarylether sulfone. U.S. patent 3,875,096, 1975.
[20] Hamza A, Chowdhury G, Matsuura T, Sourirajan S. Journal of Membrane Science 1997;129(1):55–64.
[21] Wang F, Hickner M, Kim YS, Zawodzinski TA, McGrath JE. Journal of Membrane Science 2002;197(1–2):231–42.
[22] Hickner MA, Ghassemi H, Kim YS, Einsla BR, McGrath JE. Chemical Reviews 2004;104(10):4587–611.
[23] Harrison WL, Wang F, Mecham JB, Bhanu VA, Hill M, Kim YS, et al. Journal of Polymer Science Part A: Polymer Chemistry 2003;41(14):2264–76.
[24] Li YX, VanHouten RA, Brink AE, McGrath JE. Polymer 2008;49 (13–14):3014–9.
[25] Li YX, Wang F, Yang J, Liu D, Roy A, Case S, et al. Polymer 2006;47(11):4210–7.
[26] Paul M, Park HB, Freeman BD, Roy A, McGrath JE, Riffle JS. Polymer 2008;49 (9):2243–52.
[27] Park HB, Freeman BD, Zhang Z-B, Fan G-Y, Sankir M, McGrath JE. PMSE Preprints 2006;51:889–91.
[28] Xie W, Park HB, Cook J, Lee CH, Byun G, Freeman BD, et al. Water Science and Technology 2010;61(3):619–24.
[29] Passaniti LK.Salt solubility measurements in partially disulfonated poly(arylene ether sulfone) for reverse osmosis water purification applications. Austin: The University of Texas at Austin; 2010, Master Thesis.
[30] Sagle AC, Van Wagner EM, Ju H, McCloskey BD, Freeman BD, Sharma MM. Journal of Membrane Science 2009;340(1–2):92–108.
[31] Sagle AC, Ju H, Freeman BD, Sharma MM. Polymer 2009;50(3):756–66.
[32] Wohlfarth C. CRC handbook of enthalpy data of polymer-solvent systems. Boca Raton, FL: Taylor & Francis Group; 2006.
[33] Madaeni SS, Rahimpour A. Polymers for Advanced Technologies 2005;16 (10):717–24.
[34] Zawodzinski TA, Springer TE, Davey J, Jestel R, Lopez C, Valerio J, et al. Journal of the Electrochemical Society 1993;140(7):1981–5.
[35] Wijmans JG, Baker RW. Journal of Membrane Science 1995;107(1–2):1–21.
[36] Merten U. Desalination by reverse osmosis. Cambridge: MIT Press; 1966.
[37] Paul DR. Journal of Membrane Science 2004;241(2):371–86.
[38] Van Krevelen DW, te Nijenhuis K. Properties of polymers: their correlation with chemical structure; their numerical estimation and prediction from additive group contributions. Amsterdam: Elsevier; 2009.

[39] Lonsdale HK, Merten U, Riley RL. Journal of Applied Polymer Science 1965;9:1341–62.
[40] Paul DR. Journal of Polymer Science Part B: Polymer Physics 1973;11 (2):289–96.
[41] Yasuda H, Lamaze CE, Peterlin A. Journal of Polymer Science Part B: Polymer Physics 1971;9(6):1117–31.
[42] Flory PJ. Journal of Chemical Physics 1941;9(8):660–1.
[43] Huggins ML. Journal of Chemical Physics 1941;9(5):440.
[44] Aminabhavi TM, Harlapur SF. Journal of Applied Polymer Science 1997;65 (4):635–47.
[45] Kral TE, Kuczera J, Przestalski S. Zeitschrift Fur Naturforschung C-A Journal of Biosciences 2001;56(5–6):395–401.
[46] Sun YM, Chen J. Journal of Applied Polymer Science 1994;51(10):1797–804.
[47] Zeng CY, Li JD, Li P, Chen TQ, Lin YZ, Wang D, et al. Chemical Engineering Science 2006;61(6):1892–900.
[48] Crank J. The mathematics of diffusion. Oxford: Clarendon Press; 1989.
[49] Yasuda H, Lamaze CE, Ikenberry LD. Die Makromolekulare Chemie 1968;118:19–35.
[50] Kim YS, Wang F, Hickner M, McCartney S, Hong YT, Harrison W, et al. Journal of Polymer Science Part B: Polymer Physics 2003;41(22):2816–28.
[51] Geise GM, Freeman BD, Paul DR. Polymer 2010;51(24):5815–22.
[52] Cohen MH, Turnbull D. Journal of Chemical Physics 1959;31:1164–9.
[53] Jadwin TA, Hoffman AS, Vieth WR. Journal of Applied Polymer Science 1970;14:1339–59.
[54] Geise GM, Park HB, Sagle AC, Freeman BD, McGrath JE. Journal of Membrane Science 2011;369:130–8.
[55] Ju H, Sagle AC, Freeman BD, Mardel JI, Hill AJ. Journal of Membrane Science 2010;358(1–2):131–41.
[56] Koros WJ, Fleming GK, Jordan SM, Kim TH, Hoehn HH. Progress in Polymer Science 1988;13(4):339–401.
[57] Frommer MA, Murday JS, Messalem RM. European Polymer Journal 1973;9:367–73.
[58] Robeson LM. Journal of Membrane Science 1991;62(2):165–85.
[59] Robeson LM, Burgoyne WF, Langsam M, Savoca AC, Tien CF. Polymer 1994;35 (23):4970–8.
[60] Freeman BD. Macromolecules 1999;32(2):375–80.